

# The optical design of X-Shooter for the VLT

P. Spanò<sup>\*a,b</sup>, B. Delabre<sup>c</sup>, A. Norup Sørensen<sup>d</sup>, F. Rigal<sup>e</sup>, A. de Ugarte Postigo<sup>f</sup>, R. Mazzoleni<sup>c</sup>,  
G. Sacco<sup>b</sup>, P. Conconi<sup>a</sup>, V. De Caprio<sup>a</sup>, N. Michaelsen<sup>d</sup>

<sup>a</sup>INAF-Oss. Astronomico di Brera, V. E. Bianchi 46, I-23807 Merate (LC), Italy

<sup>b</sup>INAF-Oss. Astronomico di Palermo, P.zza Parlamento 1, I-90134 Palermo, Italy

<sup>c</sup>ESO, K. Schwarzschild-str. 2, D-85748 Garching b. Muenchen, Germany

<sup>d</sup>CUO-Niels Bohr Inst., J. Maries Vej 30, DK-2100 Copenhagen, Denmark

<sup>e</sup>ASTRON, P.O. 2, 7990 AA Dwingeloo, The Netherlands

<sup>f</sup>Inst. de Astrofísica de Andalucía, C. Bajo de Huetor 50, E-18008 Granada, Spain

## ABSTRACT

The overall optical design of X-Shooter, the second generation, wide band, intermediate resolution, high efficiency, three-arms spectrograph for the VLT, is presented. We focus on the optical design of the three optimized arms, covering UVB (300-550 nm), VIS (550-1000 nm), and NIR (1000-2300 nm) wavelength ranges, including spectrographs and pre-slit optics. All spectrographs share the same original “4C” concept (Collimator Correction of Camera Chromatism). We describe also the auxiliary optics, such as dichroics, acquisition and guiding unit. Performances analysis are summarized.

Keywords: faint object spectroscopy, wide band coverage, echelle spectrograph, white pupil design, NIR spectroscopy

## 1. INTRODUCTION

X-shooter is a high-efficiency, wide band, intermediate resolution spectrograph observing simultaneously from 300 to 2300 nm (UBVRIJHK). Light from the telescope Cassegrain focal plane is wavelength-split by two dichroics and sent to three separate and optimized spectrographs through pre-slit optics.

A detailed optical analysis has been performed to validate the initial concept and verify if instrumental requirements will be fully matched. Overall description of the project is described elsewhere in these proceedings<sup>1,2</sup>.

### 1.1 Selection of the spectrograph design

Different spectrograph designs (ESI-like, UVES-like, 4C-like) have been studied during both feasibility study and preliminary design review (PDR) phases. After these efforts, a comparative analysis identified the “4C” layout<sup>3</sup> (*Collimator Compensation of Camera Chromatism*, see § 1.2) as the best option for the spectrograph layout.

Main drivers were reduced weight of the optics, reduced weight of mechanics, improvement of the stiffness, reduced costs, higher efficiency. UVB and VIS spectrographs share a very similar opto-mechanical layout. A 4C-modified layout has been developed for the NIR spectrograph to match cryogenic requirements.

Pre-slit optics has been designed around a mechanical concept for the backbone structure<sup>4</sup> where all three spectrographs will be mounted. Both UVB and VIS pre-slit arms contains an atmospheric dispersion corrector (ADC).

---

\* Email: paolo.spano@brera.inaf.it

## 1.2 The 4C concept

The idea to compensate camera chromatism through chromatic effect introduced by a Maksutov-type collimator has been proposed some years ago<sup>3</sup>. The design of the camera is considerably simplified if it does not need to be achromatized. In the 4C concept a spherical mirror gives a positive power and a dioptric diverging lens correct collimator aberrations and also introduces the negative chromatism required to compensate that of the camera. Moreover, the camera is smaller and less expensive than those required in more classical designs, like in ESI at the Keck telescope or UVES at VLT.

## 2. SPECTROGRAPHS

Figure 1 shows the optical layout of the UVB spectrograph. Light from the entrance slit, placed behind the plane of the figure, feeds an off-axis Maksutov-type collimator through a folding mirror. The collimator consists of a spherical mirror and a corrector lens (with only spherical surfaces) and is used in double pass. The collimated beam passes through a prism twice to gain enough cross-dispersion. Main dispersion is achieved through an echelle grating. After dispersion, the collimator creates an intermediate spectrum near the entrance slit, where a second folding mirror has been placed. This folding mirror acts also as field relay mirror. Then a dioptric camera (1 aspherical surface) reimages the cross-dispersed spectrum onto a tilted detector. Collimated beam size is 10cm, while camera optics are smaller than Ø80 mm.

NIR spectrograph is shown in Figure 2. The 4C concept has been modified to decrease overall size through a two-mirrors collimator. A three elements camera with mild aspherical surfaces will enhance overall efficiency, minimizing the possibility of ghosts. Cross dispersion is realized through three prisms in series, one 35° Silica prism and two 22° ZnSe prisms. Such a combination gives a dispersion more uniform than that one of a single prism, maximizing the spectral coverage for a fixed detector area.

Spectrograph main parameters are summarized in table 1.

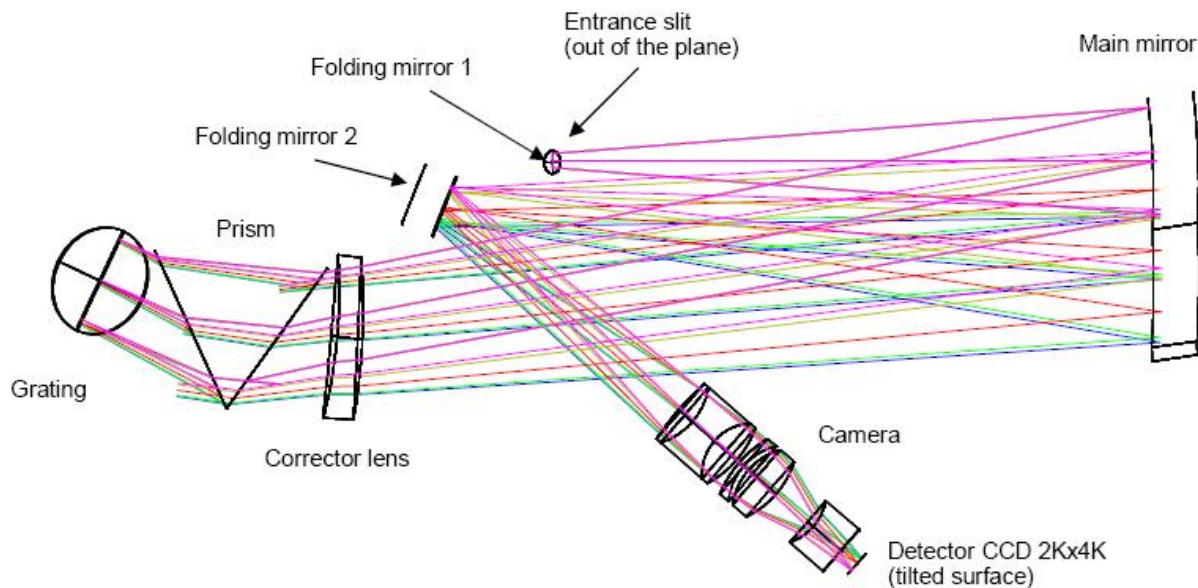


Fig. 1. The UVB spectrograph optical design. VIS arm has a very similar design. Collimated beam diameter is 10cm.

Table 1. Spectrograph main parameters.

	UVB arm	VIS arm	NIR arm
Collimator Focal Ratio	F/6.5	F/6.5	F/13.4
Slit height	12 arcsec = 3.06 mm	12 arcsec = 3.06 mm	12 arcsec = 6.36 mm
Collimated beam diameter	100 mm	100 mm	85 mm
Spectral range ( $\lambda\lambda$ )	300-550 nm	550-1000 nm	1000-2300 nm
Resolution-slit prod. ( $R\phi$ )	4500 (arcsec)	7000 (arcsec)	4500 (arcsec)
Camera free diam. (max)	80 mm	80 mm	70 mm
Camera magnification	0.41	0.42	0.2
Camera output Focal Ratio	F/2.64	F/2.7	F/2.1
Detector	4Kx2K CCD, 15 $\mu\text{m}$ pixel	4Kx2K CCD, 15 $\mu\text{m}$ pixel	2Kx1K IR array, 18 $\mu\text{m}$ pixel
Detector scale	105 $\mu\text{m}/\text{arcsec}$ (main dispersion) = 7 pixel/arcsec	111 $\mu\text{m}/\text{arcsec}$ (main dispersion) = 7 pixel/arcsec	90 $\mu\text{m}/\text{arcsec}$ (main dispersion) = 5 pixel/arcsec
Grating	180 gr/mm, 41.8° blaze angle, 2.2° off-plane angle, orders 14-24	99.4 gr/mm, 54.0° blaze angle, 2.0° off-plane angle, orders 17-30	55.0 gr/mm, 46.1° blaze angle, 1.8° off-plane angle, orders 11-26
Prism	60° Silica	49° Schott SF6	35° Infrasil + 2x22° ZnSe

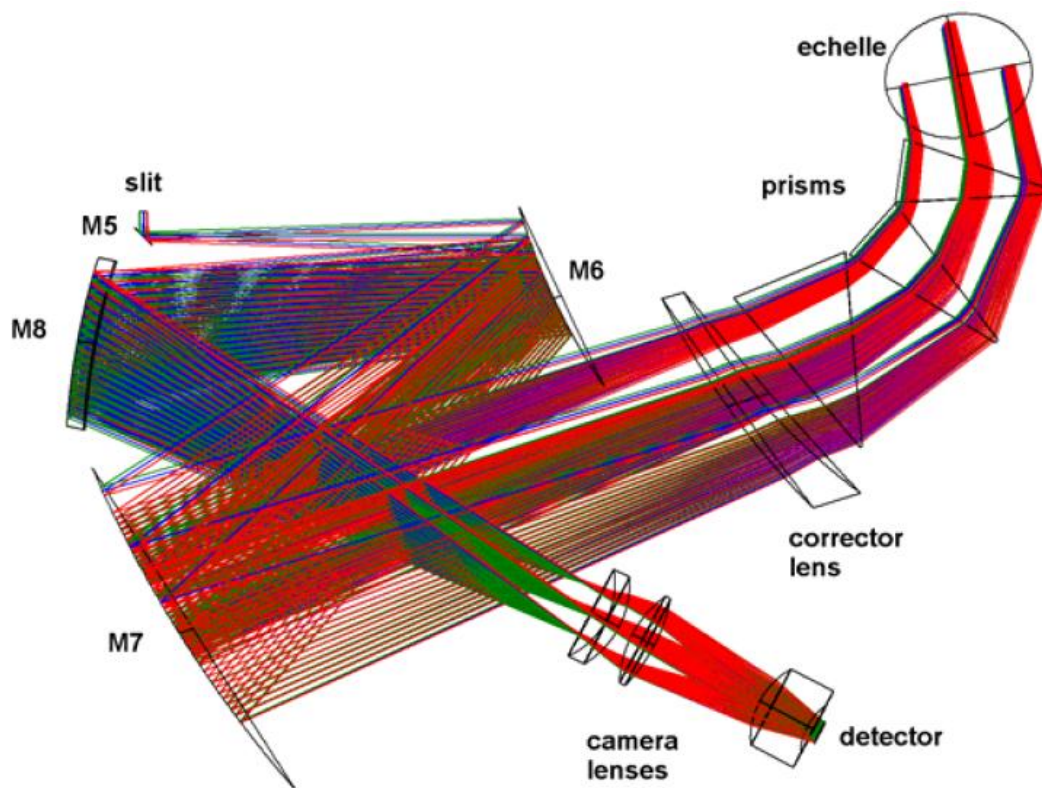


Fig. 2. NIR spectrograph layout.

## 2.1 Spectral formats

Spectral formats have been computed via ray-tracing of the optical model of each spectrograph. Spectral orders are curved. Line tilt and inter-order separation have been optimized to have enough free pixels between adjacent orders, and to ensure well calibrated reduced spectra.

Figure 3 shows a simulated ThAr spectrum.

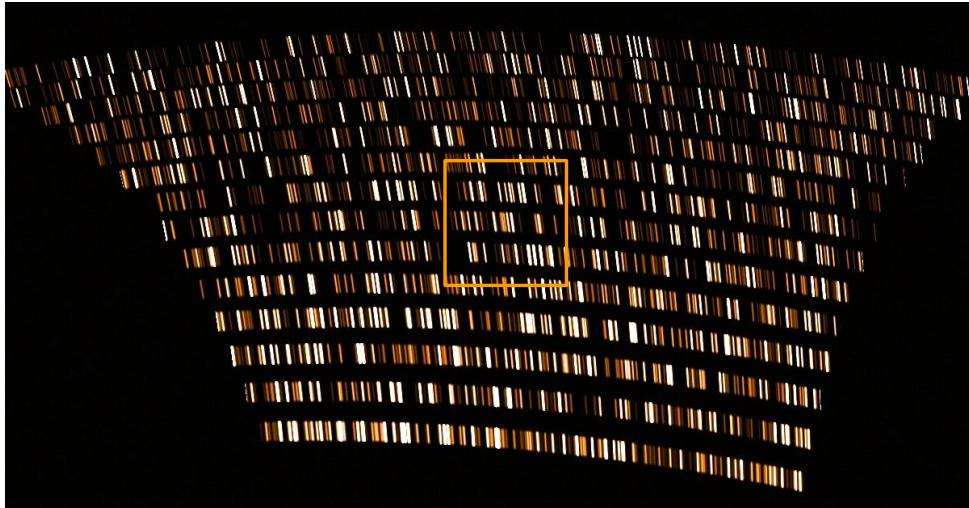


Fig. 3. Simulated ThAr spectrum in the VIS. The box shows a 500 x 500 window centered on order 24 near 680 nm.

## 2.2 Performances analysis

Extended analysis have been made to optimize overall performances, including image quality, energy concentration, sensitivity and tolerances of each optical element, thermal analysis, ghosts and stray-light analysis. Some of these analysis have driven further opto-mechanical analysis such as flexures and environmental analysis to check instrument stability.

Coatings will maximize overall efficiency. Figure 4 shows the simulated efficiency from Cassegrain focal plane to the detector (included). Table 2 summarizes average efficiency for each arm. X-Shooter will be one of the most efficient spectrographs on 8m-class telescopes, especially below 370 nm.

Table 2. X-Shooter efficiency

Spectrograph	Average blaze efficiency	Average min. efficiency
UVB	42%	22%
VIS	36%	22%
NIR	28%	16%

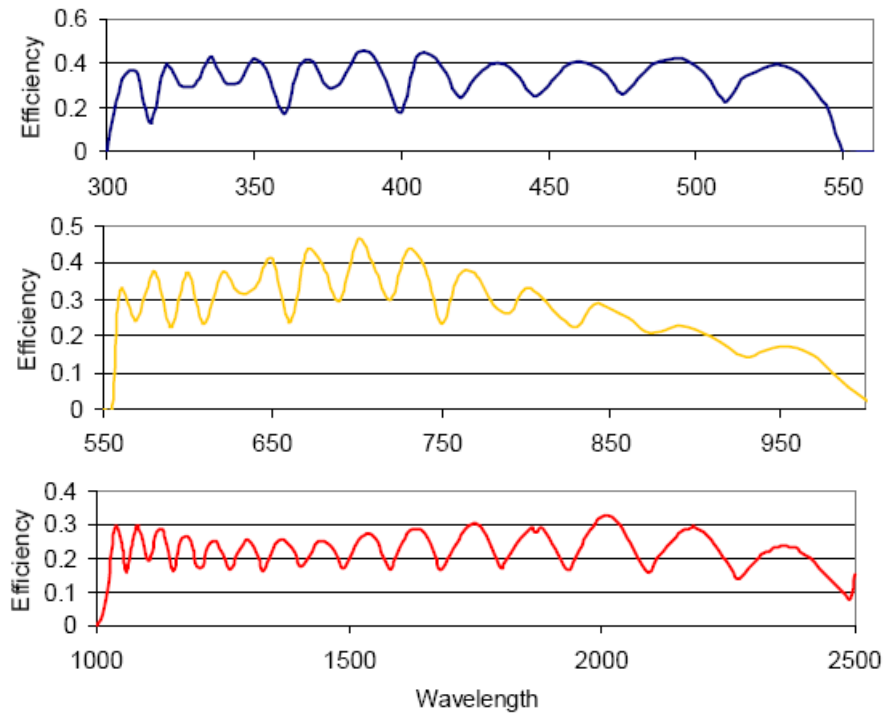


Fig. 4. Expected efficiency of UVB (top), VIS (middle), NIR (bottom) spectrograph arms from telescope focal plane to detector. Ripples are due to the grating efficiency.

### 3. RELAY OPTICS

Light from the Cassegrain focal plane feeds three different spectrographs, located onto a common backbone. Different wavelengths are split via two dichroics, placed after the Cassegrain focal plane in the divergent beam, and then different relay optics reimages the telescope focal plane onto the spectrograph entrance slits. UVB and VIS relay optics are based onto lenses, while the IR relay optics consists of only mirrors.

NIR arm will consist of four mirrors, two (one spherical, one cylindrical) will be outside the cryostat (warm optics) and will reimage telescope focal plane onto the NIR spectrograph slit, and other two flat mirrors will be inside of the cryostat (cold optics).

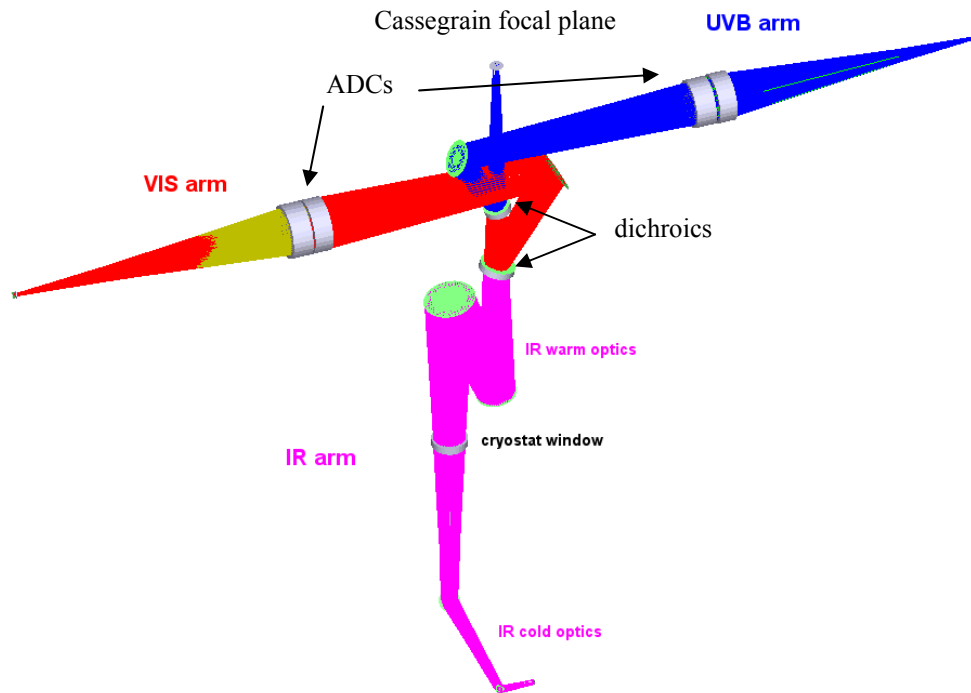


Fig. 5. The pre-slit optics.

## 2.1 Dichroics

Dichroics have been optimized to maximize efficiency in each arm, minimizing the width of the transition region. The first dichroic reflects light towards UVB spectrograph and transmits light to the VIS and NIR ones. The second dichroic reflects light towards the VIS spectrograph and transmits light to the NIR spectrograph.

## 2.2 Atmospheric Dispersion Correctors

X-Shooter suffers a very strong atmospheric dispersion due to its very wide wavelength range. Efficient correction cannot be obtained through one device only. NIR atmospheric dispersion is about 0.4 arcsec at  $60^\circ$  zenith angle, then no correction will be foreseen. Two different ADCs have been optimized for the other two arms, minimizing correction residuals having un-deviated wavelengths at 405 (UVB) and 633 (VIS) nm.

ADCs consist of two counter-rotating double prisms cemented onto two doublets, reducing air-glass interfaces. These integrated optics will act as focal reducers to match telescope and spectrograph focal ratios. Small field lenses, located near the spectrograph slits, will match pupils.

## 2.3 Slit losses

Light losses onto the entrance slit due to thermal effects (both from backbone and pre-slit optics) have been modelled. The worst case corresponds to the minimum entrance slit, that was setup at  $0.6''$ . Two cases have been considered: (a) seeing  $0.6''$  (FWHM), slit width  $0.6''$ , (b) seeing  $1''$ , slit width  $0.6''$ . A simple analytical approach gives us an estimate for the *minimum slit loss* for a perfect optical system, with the slit perfectly centred upon the PSF and extended infinitely in one direction. Slit loss is 24% for the first case, and 48% in the second one. Ray-tracing computations have

been carried out. Figure 6 shows results from this analysis. The effect of defocus is not significant at 5% level. No refocus is foreseen during observations.

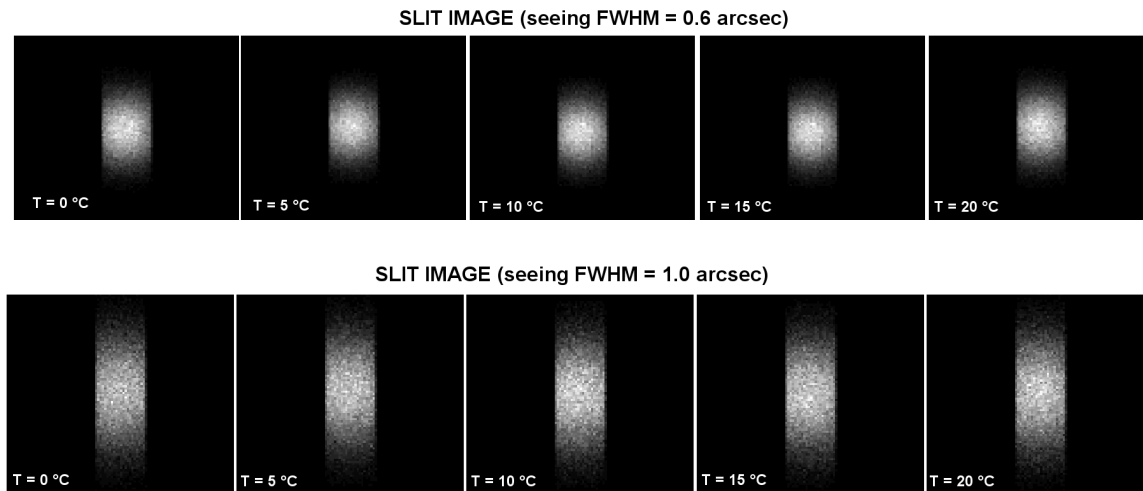


Fig.6. Illumination maps at the UVB entrance slit for different temperatures and seeing conditions.

#### 4. AUXILIARY OPTICS

##### 3.1 Acquisition and Guiding Unit

Acquisition and guiding system will implement several functions. It will allow to detect and centroid objects onto entrance slits. An artificial star (pinhole), materializing the entrance focal plane, can be placed onto the entrance focal plane for maintenance purposes. A pellicle beam splitter will allow to use the A&G camera as a slit viewing camera. Different filters will select different entrance slits. Finally, a three slices 1.8"x4" integral field unit (IFU) will be available<sup>5</sup>.

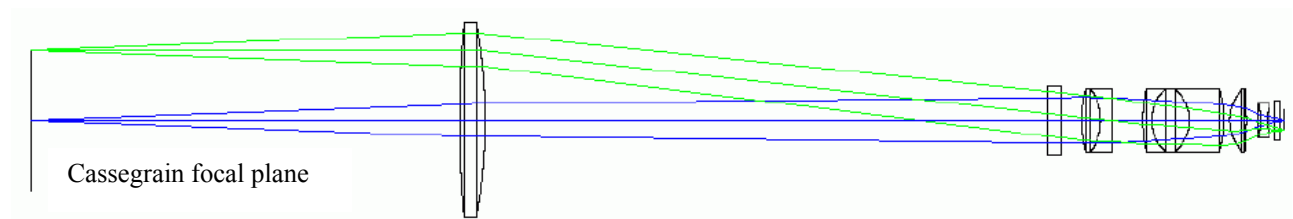


Fig. 7. Acquisition and Guiding camera optical layout.

##### 3.2 Pupil viewer

A pupil imager would be convenient, not only for aligning the A&G camera, but also for aligning the arms of the spectrograph by using the slit viewer pellicle. Two lenses are required: one placed on the A&G side of the pellicle, and one on the A&G filter wheel. To view each of the three spectrograph pupils, a lens and filter sandwich is selected in the A&G filter wheel. The same pellicle lens can be used for all three arms.

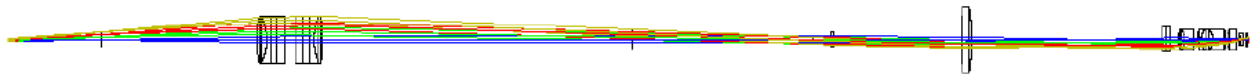


Fig. 8. Pupil viewing optics.

### 3.3 Dichroic viewer

An increase in infrared background can be expected due to dust settling on the first dichroic (DC1). The amount of dust on DC1 can be monitored by using the slit viewing pellicle and focusing the A&G camera on DC1 by inserting optics (lens/filter) in the filter wheel.

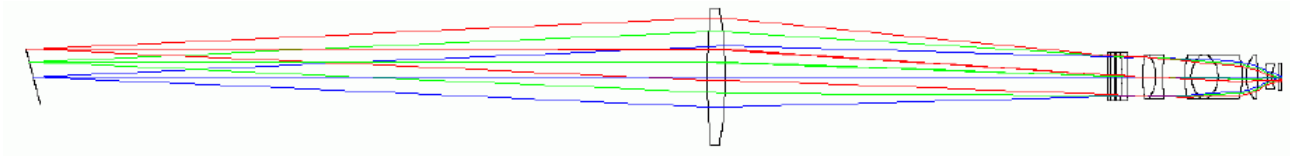


Fig. 9. The A&G camera acting as dichroic viewer.

## REFERENCES

1. S. D'Odorico, et al.:2004, SPIE 5492, 220
2. S. D'Odorico, et al.: 2006, these proceedings
3. B. Delabre, H. Dekker, S. D'Odorico, F. Merkle: 1989, SPIE 1055
4. N. Michaelsen, et al.: 2006, these proceedings
5. I. Guinouard, et al.: 2006, these proceedings